

# Pressure- and Heat-Induced Insertion of CO<sub>2</sub> into an Auxetic Small-Pore Zeolite

Yongjae Lee,<sup>\*,†</sup> Dan Liu,<sup>†</sup> Donghoon Seoung,<sup>†</sup> Zhenxian Liu,<sup>‡</sup> Chi-Chang Kao,<sup>§</sup> and Thomas Vogt<sup>||</sup>

<sup>†</sup>Department of Earth System Sciences, Yonsei University, Seoul, 120749, Korea

<sup>‡</sup>Geophysical Laboratory, Carnegie Institution of Washington, Washington, D.C. 20015, United States

<sup>§</sup>Stanford Synchrotron Radiation Lightsource, SLAC National Accelerator Laboratory, Menlo Park, California 94025-7015, United States

<sup>||</sup>NanoCenter & Department of Chemistry and Biochemistry, University of South Carolina, Columbia, South Carolina 29208, United States

**S** Supporting Information

**ABSTRACT:** When the small-pore zeolite natrolite is compressed at ca. 1.5 GPa and heated to ca. 110 °C in the presence of CO<sub>2</sub>, the unit cell volume of natrolite expands by 6.8% and ca. 12 wt % of CO<sub>2</sub> is contained in the expanded elliptical channels. This CO<sub>2</sub> insertion into natrolite is found to be reversible upon pressure release.

Insertion of CO<sub>2</sub> into micro- and mesoporous materials has focused on large-pore zeolites,<sup>1</sup> metal–organic frameworks (MOFs),<sup>2</sup> and zeolitic imidazole frameworks (ZIFs)<sup>3,4</sup> since these materials might find use as both capture and storage media.<sup>5</sup> Small-pore zeolites, though generally limited in gas adsorption properties, might be used as alternate hosts for CO<sub>2</sub> storage considering their enhanced thermal and mechanical stability. Natrolite is one of the small-pore zeolites featuring elliptical 8-ring channels filled with sodium cations and water molecules in a 1:1 ratio at ambient conditions.<sup>6–8</sup> When the water molecules are removed, however, the ellipticity of the 8-ring channel increases further and as a consequence CO<sub>2</sub> adsorption becomes sterically hindered.<sup>9,10</sup> It has been recently shown that the natrolite framework is auxetic and under pressure enlarges the opening and reduces the ellipticity of its 8-ring channels thereby allowing (selective) adsorption of water or argon present in the hydrostatic pressure medium.<sup>11–14</sup> We have investigated whether this small-pore zeolite natrolite can also become an adsorbent and storage medium for other gases under suitable high-pressure and -temperature conditions.

The kinetic diameter of CO<sub>2</sub> with 3.3 Å is slightly smaller than that of argon given as 3.5 Å<sup>15</sup> or 3.7 Å.<sup>16</sup> We therefore would expect to be able to insert CO<sub>2</sub> under pressure and temperature into the natrolite channels. In this work we show that this can be done at 1.5(1) GPa and 110 °C,<sup>17</sup> conditions quite similar to those required to insert argon<sup>14</sup> and determine the structural arrangements of the CO<sub>2</sub> molecules in natrolite. A high-pressure synchrotron X-ray powder diffraction study<sup>17</sup> shows that the natrolite unit cell expands by 6.8% near 1.5 GPa when heated and takes up CO<sub>2</sub> molecules from the pressure medium. When the pressure is released, the expanded unit cell is initially recovered,

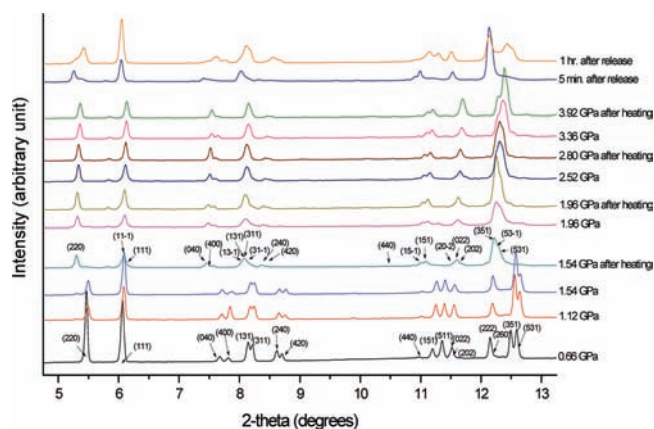


**Figure 1.** Pressure- and temperature-induced changes in the synchrotron X-ray powder diffraction patterns measured for natrolite under CO<sub>2</sub> medium using an imaging plate detector ( $\Delta d/d \approx 10^{-2}$ ) at the beamline 5A at the Pohang Accelerator Laboratory. Note that two phases are mixed after pressure release (upper two patterns). Miller indices are shown for the selected Bragg peaks.

and complete equilibration takes about 1 h. This process is also confirmed by the changes in the lattice vibration modes based on micro-Raman measurements.

Pressure-dependent changes in the observed synchrotron X-ray powder diffraction patterns from each run are shown in Figure 1. Visual inspection of the diffraction patterns reveals that the lattice expansion of the natrolite occurs at 1.54(5) GPa after heating, and the expanded phase persists after the pressure is released and the sample is exposed to the atmosphere, at least for 1 h.

Pressure-dependent changes of the unit cell lengths and volume of natrolite in the presence of CO<sub>2</sub> are shown in Figure 2. The sample sealed with solid CO<sub>2</sub> at low temperatures was found to be at a pressure of 0.66(5) GPa at room temperature. As the pressure increases, the unit cell volume contracts gradually up to 1.54(5) GPa. The volume contraction of natrolite observed under CO<sub>2</sub> pressure is larger compared to the one observed in

Received: October 30, 2010

Published: January 26, 2011

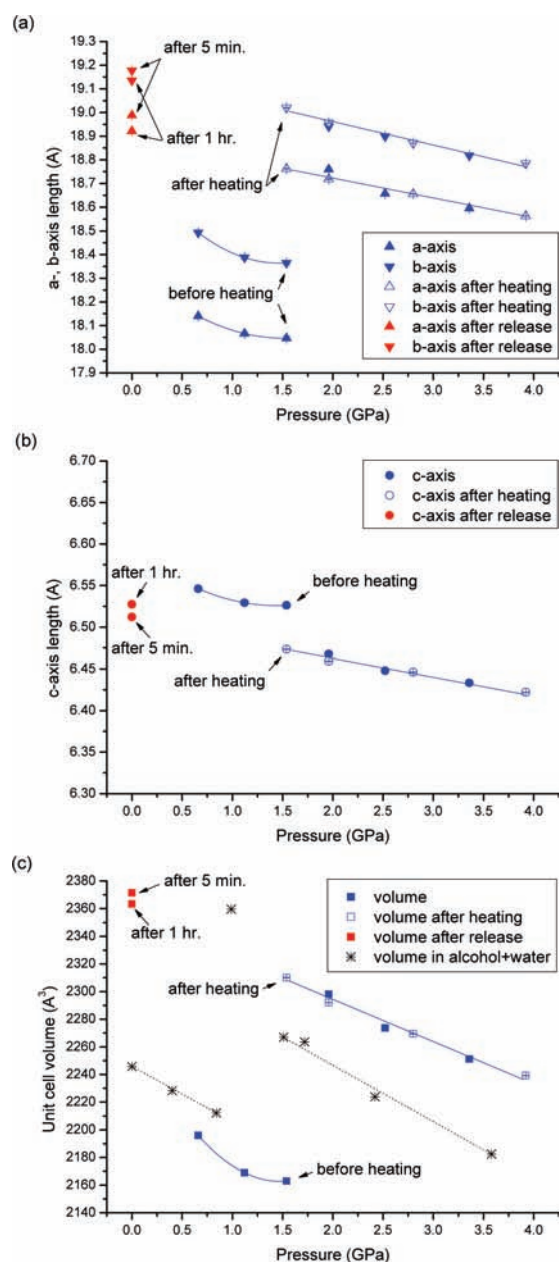


**Figure 2.** Pressure-dependent changes in the (a, b) refined unit cell lengths and (c) volume of natrolite under  $\text{CO}_2$  pressure medium (filled blue symbols, upon pressure increase; open blue symbols, after heating; and filled red symbols, after pressure release). The changes in the unit cell volume are also compared to the previous results (black asterisks) from the alcohol + water mixture medium run (methanol/ethanol/water in 16:3:1 by volume).

our previous study using alcohol and water mixtures as a pressure-transmitting medium (Figure 1c).<sup>12</sup> This is interpreted to be partly due to the fact that the alcohol and water mixture is known to exert hydrostatic pressure below ca. 1.5 GPa whereas  $\text{CO}_2$  is in its critical state in this region and has a larger kinetic diameter than  $\text{H}_2\text{O}$ .<sup>18</sup> After the measurement at 1.54(5) GPa, the DAC was placed in an oven at 110 °C for 1 h and allowed to cool back to room temperature. A subsequent measurement after this heating revealed that the sample pressure had not been affected and the unit cell volume of natrolite had expanded by 6.8%. This expansion is close to the 7.0% observed in the natrolite to

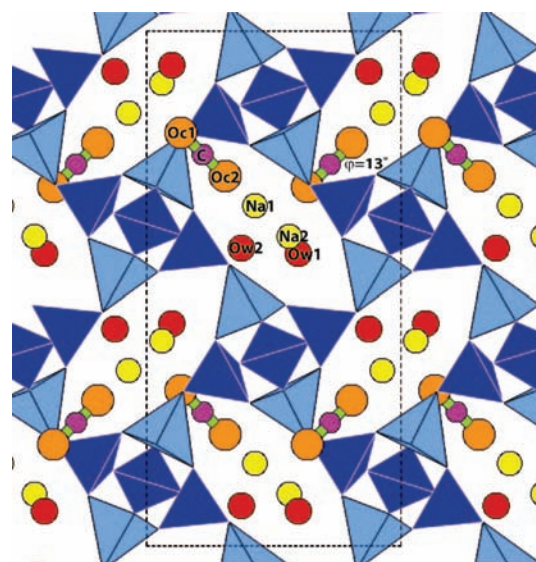


**Figure 3.** A polyhedral representation of  $\text{CO}_2$ -inserted natrolite formed at 1.54(5) GPa after heating, viewed along [001], the chain/channel axis. Note that the  $\text{CO}_2$  molecules lie on the plane perpendicular to the channel axis, tilted by  $\varphi = 13^\circ$ . Dark (light) tetrahedra illustrate an ordered distribution of Si (Al) atoms in the framework.

ordered-paranatrolite transition near 1 GPa in the presence of the alcohol–water medium.<sup>19</sup>

A structural model of natrolite at 1.54(5) GPa after heating was refined against X-ray powder diffraction data using the monoclinic  $Cc$  space group and revealed that  $\text{CO}_2$  molecules had been inserted into the natrolite channels (Figure 3). The refined unit cell formula of the  $\text{CO}_2$ -inserted natrolite formed at 1.54(5) GPa after heating is  $\text{Na}_{16}\text{Al}_{16}\text{Si}_{24}\text{O}_{80} \cdot 16.0\text{H}_2\text{O} \cdot 8\text{CO}_2$ , which indicates ca. 12 wt % of  $\text{CO}_2$  loading into natrolite. Yaghi et al. found an 8.9 wt % loading in Mg-MOF-74.<sup>2</sup> In commercial treatments of natural gas a 30% monoethanolamine solution can take up 13.4 wt.%  $\text{CO}_2$ .<sup>20</sup> After  $\text{CO}_2$  insertion, the elliptical channels have a more circular shape due to the smaller chain rotation angle  $\psi$  which decreased from ca.  $25^\circ$  at ambient conditions to ca.  $20.5^\circ$ .<sup>6</sup> The inserted  $\text{CO}_2$  molecules lie on the plane perpendicular to the channel, tilted by ca.  $\varphi = 13^\circ$ . The distribution of nonframework sodium cations remains intact in the presence of  $\text{CO}_2$  in the channel, whereas the water molecules migrate to one side of the channel. These water molecules bridge the sodium chain along the channel with interatomic distances in the range of 2.20(6) and 2.94(6) Å (Supporting Information). The oxygen atoms of the inserted  $\text{CO}_2$  molecules indicate interactions with the sodium cations and the oxygen atoms from the water molecules and the framework with the coordination distances in the range of 2.41(6)–2.58(7) Å and 2.70(6)–3.12(7) Å, respectively. Overall, the OC1 and OC2 oxygen atoms of the inserted  $\text{CO}_2$  molecules form a helical arrangement together with the OW1 and OW2 oxygen atoms from the water molecules and confine the sodium cations along the channel.

High-pressure  $\text{CO}_2$  insertion into natrolite was also monitored using a customized micro-Raman microscope equipped with a 532 nm laser in a back-scattering geometry with a resolution of about  $1 \text{ cm}^{-1}$ . As in the diffraction experiments, pure water was used as a pressure medium in run #1 and solid  $\text{CO}_2$  in run #2. The observed changes in the Raman spectra of natrolite in run #1 show close agreement with the previously

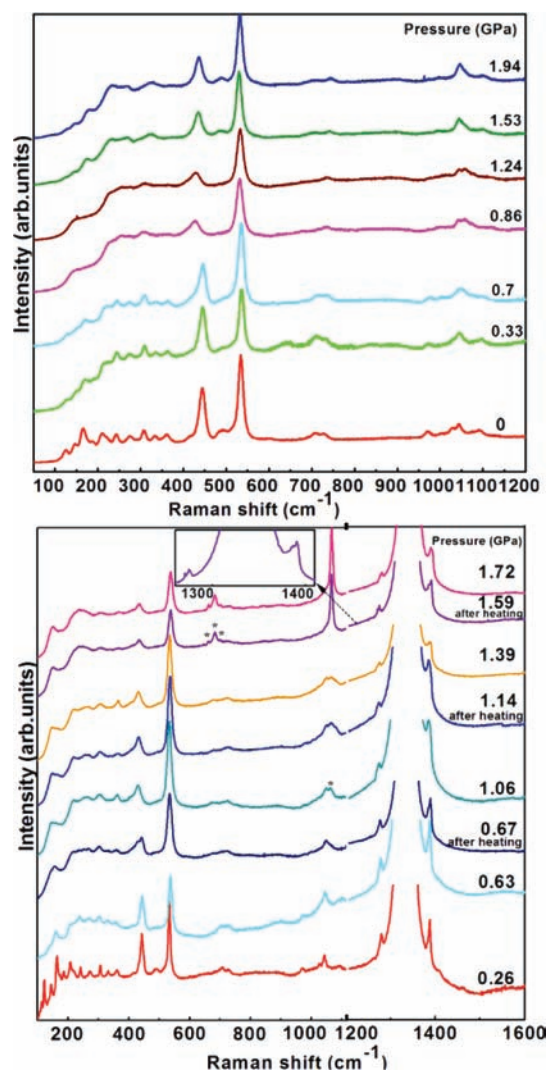


**Figure 4.** Pressure-dependent changes in the Raman spectra of natrolite under water pressure medium (upper) and CO<sub>2</sub> pressure medium (lower). An inset in the lower figure emphasizes the splittings of the  $\nu^-$  and  $\nu^+$  vibrational modes of CO<sub>2</sub>.

established spectroscopic and crystallographic results (Figure 4, upper).<sup>19,21</sup> Two successive phase transitions are indicated by the abrupt changes in the helical 8-ring frequency mode near 443 cm<sup>-1</sup> showing a large red shift at 0.86(5) GPa and an opposite shift at 1.53(5) GPa. This is associated with the volume expansion and contraction to form the ordered-paranatrolite and superhydrated natrolite in the presence of water, respectively.<sup>19</sup> In run #2, the presence of CO<sub>2</sub> as a pressure medium is visible by the additional Raman peaks at 1282 and 1387 cm<sup>-1</sup>, which stem from  $\nu^-$  (the Fermi resonance of the overtone CO<sub>2</sub> bending mode,  $2\nu_2$ ) and  $\nu^+$  (the symmetric stretching mode,  $\nu_1$ ), respectively (Figure 4, lower).<sup>22</sup>

As the pressure increases, the low-frequency lattice modes become progressively weaker and broader as the CO<sub>2</sub> medium becomes a nonhydrostatic medium. At 1.06(5) GPa, a new Raman band starts to be seen close to the stretching vibrational mode of the TO<sub>4</sub> tetrahedra near 1065 cm<sup>-1</sup>. At 1.59(5) GPa after heating, this new band increases and sharpens, and three new Raman bands emerge near 680 cm<sup>-1</sup>. These features result from the observed monoclinic distortion of the natrolite

framework and the concomitant insertion of CO<sub>2</sub> molecules into the channel. After the CO<sub>2</sub> insertion, both the  $\nu^-$  and  $\nu^+$  vibrational modes of CO<sub>2</sub> appear to split indicating two different conformations of the CO<sub>2</sub> molecules, i.e., one in the pressure medium and the other inside the natrolite channels (Figure 4, lower).

In summary, we have demonstrated that under pressure and elevated temperatures CO<sub>2</sub> can be inserted into the small-pore zeolite natrolite. The inserted CO<sub>2</sub> molecules show strong interactions with both the framework and nonframework species and are found to be fully recoverable an hour after pressure release. Chemical and structural modifications of the natrolite structure can be made in order to modify the insertion conditions and allow use in CO<sub>2</sub> capture and storage technologies.

## ASSOCIATED CONTENT

**S Supporting Information.** Crystallographic and spectroscopic data. This material is available free of charge via the Internet at <http://pubs.acs.org>.

## AUTHOR INFORMATION

### Corresponding Author

YongjaeLee@yonsei.ac.kr

## ACKNOWLEDGMENT

This work was supported by the Global Research Laboratory program of the National Research Foundation of the Korean Government. Y.L. acknowledges the support from the Nuclear R&D Program of the NRF to build the micro-Raman system used in this study. The authors thank Dr. Hyun-Hwi Lee for the operation of the SA beamline at Pohang Accelerator Laboratory (PAL). Experiments at PAL were supported in part by the MEST and POSTECH.

## REFERENCES

- Breck, D. W. *Zeolite Molecular Sieves*; Krieger: Malabar, FL, 1984.
- Britt, D.; Furukawa, H.; Wang, B.; Glover, T. G.; Yaghi, O. M. *Proc. Natl. Acad. Sci. U.S.A.* **2009**, *106*, 20637–20640.
- Furukawa, H.; Ko, N.; Go, Y. B.; Aratani, N.; Choi, S. B.; Choi, E.; Yazaydin, Ö.; Snurr, R. Q.; O’Keeffe, M.; Kim, J.; Yaghi, O. M. *Science* **2010**, *329*, 424–428.
- Millward, A. R.; Yaghi, O. M. *J. Am. Chem. Soc.* **2005**, *127*, 17998–17999.
- D’Alessandro, D. M.; Smit, B.; Long, J. R. *Angew. Chem., Int. Ed.* **2010**, *49*, 6058–6082.
- Baur, W. H.; Kassner, D.; Kim, C.-H.; Sieber, N. H. *Eur. J. Mineral.* **1990**, *2*, 761–769.
- Pauling, L. *Proc. Natl. Acad. Sci. U.S.A.* **1930**, *16*, 453–459.
- Taylor, W. H.; Meek, C. A.; Jackson, W. W. *Z. Kristallogr.* **1933**, *84*, 373–398.
- Baur, W. H.; Joswig, W. N. *Jb. Miner. Mh.* **1996**, 171–187.
- Shin, J.; Cambor, M. A.; Woo, H. C.; Miller, S. R.; Wright, P. A.; Hong, S. B. *Angew. Chem., Int. Ed.* **2009**, *48*, 1–4.
- Belitsky, I. A.; Fursenko, B. A.; Gubada, S. P.; Kholdeev, O. V.; Seryotkin, Y. V. *Phys. Chem. Minerals* **1992**, *18*, 497–505.
- Lee, Y.; Vogt, T.; Hriljac, J. A.; Parise, J. B.; Artioli, G. *J. Am. Chem. Soc.* **2002**, *124*, 5466–5475.
- Gatt, R.; Zammit, V.; Caruana, C.; Grima, J. N. *Phys. Status Solidi B* **2008**, *245*, 502–510.
- Lee, Y.; Hriljac, J. A.; Vogt, T. *J. Phys. Chem. C* **2010**, *114*, 6922–6927.

(15) Müller, U.; Reichert, H.; Robens, E.; Unger, K. K.; Grillet, Y.; Rouquerol, F.; Rouquerol, J.; Pan, D.; Mersmann, A. *Fresenius' J. Anal. Chem.* **1989**, 333, 433–436.

(16) Pillaia, R. S.; Petera, S. A.; Jasra, R. V. *Microporous Mesoporous Mater.* **2008**, 113, 268–276.

(17) The mineral natrolite (ideal formula  $\text{Na}_{16}\text{Al}_{16}\text{Si}_{24}\text{O}_{80} \cdot 16.0\text{-H}_2\text{O}$ , from Argentina, OBG International) was used in this study. High-pressure  $\text{CO}_2$  insertion into natrolite was monitored in situ using a Merrill-Bassett type diamond-anvil cell (DAC) and monochromatic synchrotron X-ray powder diffraction at the 5A-HFMS beamline at Pohang Accelerator Laboratory (PAL). The powdered sample of natrolite was loaded into a 200  $\mu\text{m}$  diameter stainless steel gasket chamber together with some ruby chips for in situ pressure measurements. The cell was cooled by partially immersing both the upper and lower blocks of the DAC in a liquid nitrogen bath, and small chunks of pure dry ice were loaded into the sample chamber before closing the DAC. After the DAC was brought to room temperature, its internal pressure was measured by analyzing the shift in the R1 emission line of the included ruby chips (precision:  $\pm 0.05$  GPa). The natrolite and  $\text{CO}_2$  mixture in the DAC was equilibrated for about 30 min at each measured pressure, and the pressure was increased in ca. 0.5 GPa increments. From 1.54(5) GPa on, the measurements were repeated twice after heating the DAC ex situ in an oven. For the last two pressure points of 2.52(5) and 3.36(5) GPa, the sample pressure was found to be increased after the ex situ heating procedure to 2.80(5) and 3.92(5) GPa, respectively. In all our measurements supercritical  $\text{CO}_2$  is present in the DAC and the heating should only affect the pore opening of the framework to further facilitate the insertion of  $\text{CO}_2$ . The structural refinements were performed using the Rietveld method and the GSAS suite of programs.<sup>23,24</sup> The refined structural model at 1.54(5) GPa after heating is also summarized in the Supporting Information.

(18) Hazen, R. M.; Finger, L. W. *Comparative Crystal Chemistry*; John Wiley & Sons: New York, 1982.

(19) Lee, Y.; Hriljac, J. A.; Parise, J. B.; Vogt, T. *Am. Mineral.* **2005**, 90, 252–257.

(20) Walton, K. S.; LeVan, M. D. *Sep. Sci. Technol.* **2006**, 41, 485–500.

(21) Goryainov, S. V.; Smirnov, M. B. *Eur. J. Mineral.* **2001**, 13, 507–519.

(22) Olijnyk, H.; Daufer, H.; Jodl, H. J.; Hochheimer, H. D. *J. Chem. Phys.* **1988**, 88, 4204–4212.

(23) Rietveld, H. M. *J. Appl. Crystallogr.* **1969**, 2, 65–71.

(24) Larson, A. C.; VonDreele, R. B. "GSAS; General Structure Analysis System," Report LAUR 86-748, Los Alamos National Laboratory, NM, 1986.